# Moiré Interference in Gamma Camera Quality Assurance Images

Graham Charles Hart

*Department of Medical Physics, Bradford Royal Infirmary, West Yorkshire, England*

Moiré interference effects have been noted in gamma camera images for some time. Recent work has shown that the effects are still prevalent with the current generation of cameras, though apparently dependent upon collimator design. All previous work has been related to bar phantom images only. This paper also demonstrates a variety of moiré effects using the Anger "pie" phantom. Some of the principles underlying moiré interference as they apply to gamma cameras are given and possible uses of the effects are discussed, as well as the limitations they impose upon the use of certain test objects in routine quality assurance testing.

**J Nucl Med 27:820–823, 1986**

Moiré interference in gamma camera images was first recognized and reported in 1971 (*1*), with further observations on the effects in 1972 and 1979 (*2,3*). At first it was thought that the moiré effect was at its most prominent in systems of poor spatial resolution, and with the larger holes and thicker septa of medium energy collimators. Other work at this time (*4,5*), however, suggested that the moiré effect should be visible using low-energy collimators as the intrinsic spatial resolution of gamma cameras improved.

This has recently been confirmed (*6*), with the further observation that the effect is dependent upon the design of the collimators being used. Currently moiré fringes are only seen with "hole-array" collimators, that is, ones constructed as a hexagonal close-packed array of holes in a solid lead block. No fringes have as yet been observed with the other routinely used type of collimator, constructed using folded "zig-zag" ribbons of lead separated by lead strips. The reasons for this have been discussed elsewhere (*6*).

Previously published work has dealt exclusively with effects arising from the use of bar phantoms in quality assurance images. This paper, as well as demonstrating the different types of moiré interference present in bar phantom images, will also show how such effects can be seen in Anger "pie" phantom images. It will give some of the theoretical background to the effects, discuss the way they may best be utilized and the limitations they impose upon the use of certain test objects.

Received Aug. 8, 1985; revision accepted Jan. 15, 1986.

For reprints contact: Graham Charles Hart, Dept. of Medical Physics, Bradford Royal Infirmary, Duckworth Lane, Bradford BD9 6RJ, West Yorkshire, England.

## The Nature of Moiré Interference (*7,8*)

Moiré interference arises when one family of curves is superimposed upon another. The loci of the points of intersection of the two families of curves form a new family of curves known as the moiré pattern.

Any regular curvilinear pattern may be used for the two interacting curve families, usually known as gratings. Unlike most interference effects, that only occur over distances of the same order of magnitude as the wavelength of the radiation, moiré effects can be observed using relatively coarse gratings at centimeter level and above.

In practice, many different types of grating are used ranging from radial and circular gratings to arrays of lines usually orthogonal but infrequently hexagonal. The most common type of grating, however, is undoubtedly the line grating, ideally composed of parallel equispaced opaque bars of constant width separated by transparent slits of equal width. The distance between the edge of a bar or slit and the corresponding edge of the next bar or slit in such a grating is usually known as the pitch of the grating.

Two types of moiré interference are commonly observed. The first and most common is where two gratings of equal pitch are angularly displaced, when the gratings will be traversed by a number of equidistant fringes, the pitch of which decreases as the angle of relative displacement increases. The fringes make an angle which bisects the perpendiculars from the two interfering gratings.

The second type of moiré interference occurs when two gratings of slightly different pitch are aligned parallel to each other. In this case fringes occur in a direction parallel to the gratings, the pitch of the fringes increasing as the difference in pitch of the two gratings decreases.

Although in both of the above examples the pitches of the two gratings are approximately equal, both kinds of moiré effect also occur if the pitches of the gratings are to a close approximation in the ratio of two small integers, i.e., 2:1, 3:2.

The mathematic analysis of moiré interference has been extensive, and formulae have been developed for most of the commonly used gratings to give the interfringe spacing and fringe angle over all possible circumstances.

For two line gratings of pitch p and $p(1 + \lambda)$, where $\lambda$ is a small quantity, that are displaced by an angle $\theta$, the interfringe spacing f is given by:

$$f = p(1 + \lambda)\cdot(\lambda^2 \cos^2 \theta/2 + (2 + \lambda)^2 \sin^2 \theta/2)^{-1/2}$$

and the fringe angle $\phi$ is given by:

$$\sin \phi = \sin \theta\cdot(\lambda^2 \cos^2 \theta/2 + (2 + \lambda)^2 (\sin^2 \theta/2))^{-1/2}.$$

If the two gratings are identical, then $\lambda = 0$, and the equations may be simplified to:

$$f = p/(2\sin \theta/2) \quad \text{and} \quad \sin \phi = \cos \theta/2.$$

From these equations it can be seen that small changes in the angle $\theta$ can result in larger changes in the interfringe spacing, and that the fringe angle does indeed bisect the supplementary angle of angle $\theta$.

For two parallel nonidentical gratings, the angle $\theta = 0$ and the equations reduce to:

$$f = p(1 + \lambda)/\lambda \quad \text{and} \quad \sin \phi = 0,$$

and hence such fringe systems will be parallel to the direction of the gratings.

### The Effect of Moiré Interference

Moiré interference can readily be observed in both bar and Anger phantom images using high sensitivity and general purpose collimators of the hole-array type.

*Bar phantom.* The bar phantom used in the images here was a transmission-type consisting of six sets of parallel lead bars with unit bar width/space ratios, set in perspex. The sizes of the bars were 5.0, 4.0, 3.5, 3.0, 2.5, and 2.0 mm.

Figure 1 shows an image of the phantom with technetium-99m ($^{99m}$Tc) containing $10^6$ counts using the high sensitivity collimator, with the bars angled at ~45° to the principal axis of the collimator, which in this and all subsequent images runs vertically down the image. The first two segments show real bar images, the third has a mixture of real bar and moiré interference, and the last three segments show clear moiré fringes only.

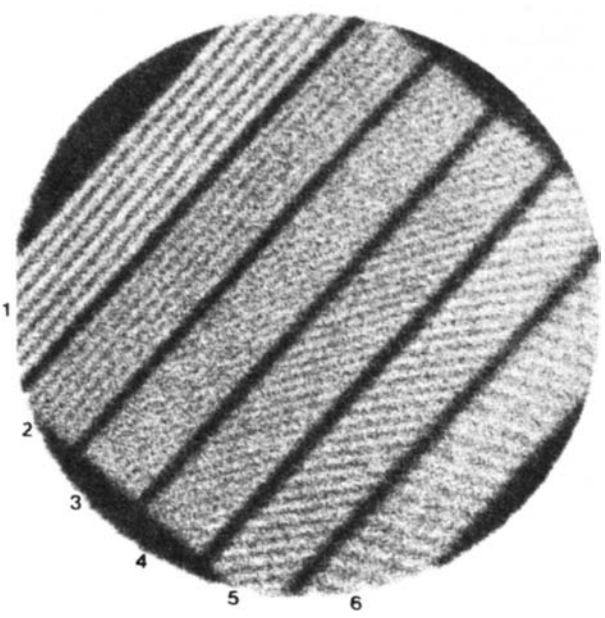


**FIGURE 1**
Bar phantom image with high sensitivity collimator, bars 45° angle to axis of collimator. Segments of decreasing size labeled 1–6

This interference, of the first type, shows how the fringe angle increases as the sizes of the bars decrease.

Moiré interference of the second type can be seen clearly in Fig. 2, this time using a high sensitivity converging collimator, again with $10^6$ counts. Here the

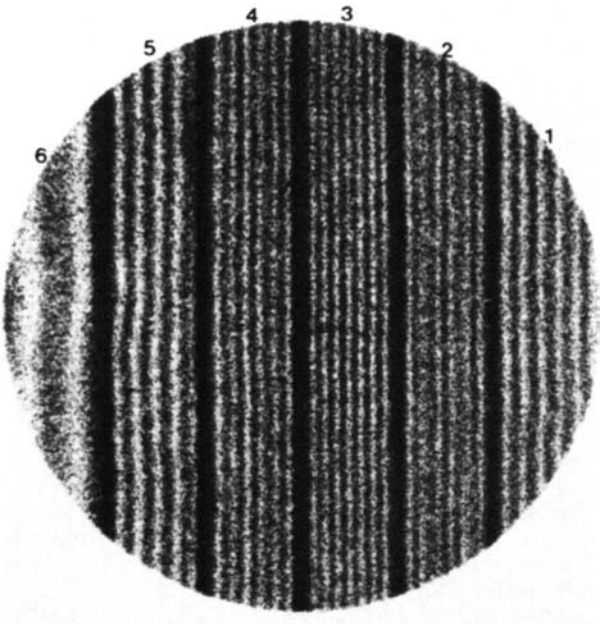


**FIGURE 2**
Bar phantom image with high sensitivity collimator; bars parallel to axis of collimator

bars are closely aligned with the axis of the collimator and hence the fringe systems will lie in the same direction. The first and possibly second segments from the right are real bar images, but subsequently moiré effects take over, with sharp fringes of increasing size as the bars become narrower.

*Anger phantom.* Two different types of moiré interference can be seen in the Anger phantom images below (Figs. 3–5). All the images were made with a cobalt-57 flood source, $10^6$ counts, and a standard design phantom with six sets of holes from 4.0 mm down to 1.5 mm in 0.5 mm steps. The hole spacing is four times the hole diameter in each segment.

The first image, Fig. 3, taken using the high sensitivity converging collimator, shows segments one to three with the correct hole pattern. Segment four apparently shows some holes correctly, but with an overlaid moiré interference pattern of larger hexagons. Segment five shows generalized destructive interference, but the sixth segment has lines of holes of incorrect size and alignment, recognized because the holes no longer run parallel to the edges of the segment and are larger than would be expected. This is a moiré effect analogous to the first type seen in the bar phantom images.

The next image, Fig. 4, again with the high sensitivity converging collimator, has the phantom rotated to a new position. In this position, ~78° from the position of Fig. 3, only the first two segments are free of moiré interference effects. Segment three has holes again overlaid with the larger hexagonal fringes. The fourth segment shows severe distortion over its entirety, and segments five and six are composed of incorrectly sized and aligned holes, increasing in size as the holes in the phantom decrease. These are again interference effects of the first type. In fact, the fifth segment has a faint overlaid hexagonal fringe pattern of the same size but different orientation as that in the third segment.

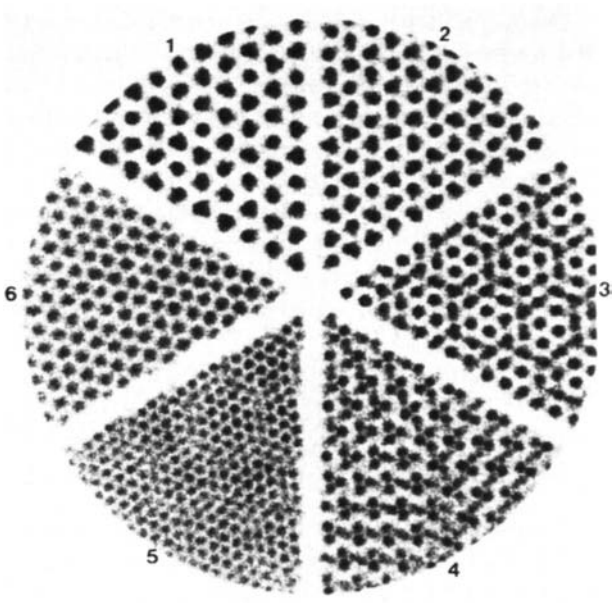


**FIGURE 4**
Anger phantom image with converging collimator, rotated ~78° clockwise with respect to Fig. 3

Figure 5 shows the phantom used with a general purpose collimator. The finer holes permit four seg-

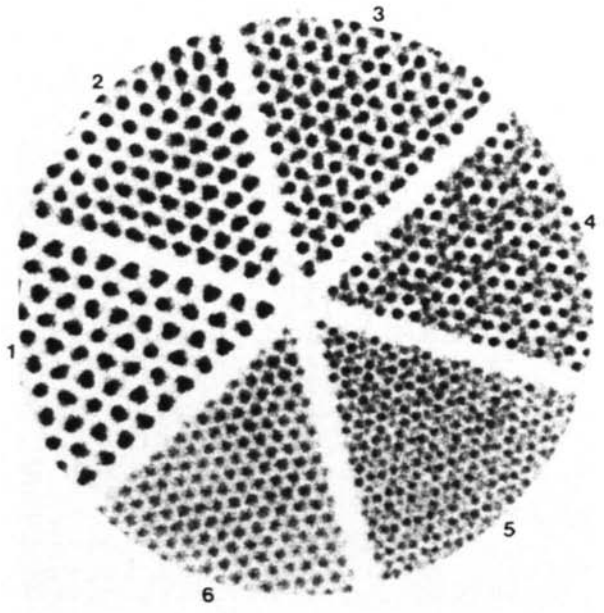


**FIGURE 3**
Anger phantom image with converging collimator

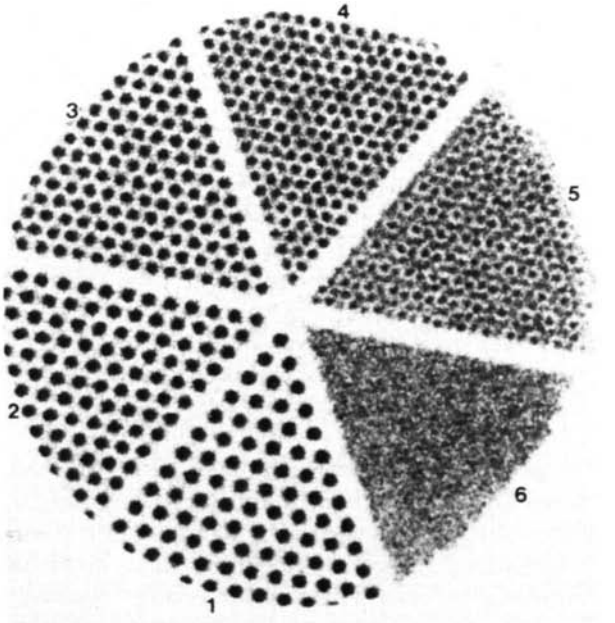


**FIGURE 5**
Anger phantom image with general purpose collimator

ments to be resolved, though with a faint hexagonal fringe in the fourth segment. The fifth segment is composed entirely of small hexagonal fringes, with the sixth segment unresolved.

## DISCUSSION

The preceding images show the extent to which moiré interference effects disrupt both bar and Anger phantom images. These effects are most evident in images using the different types of high sensitivity collimator, though are still visible with general purpose collimators.

In bar phantom images line fringe effects result from interference between the lead bars and the "lines" of lead forming the septa. In the Anger phantom hexagonal fringe effects are seen from interference between the two hexagonal close-packed arrays of holes in the phantom and collimator. A secondary, more subtle, interference effect also occurs between the lines of holes in both phantom and collimator, thus producing a fringe also composed of lines of holes, the size and alignment of which are dependent upon their relative orientations.

It can be seen that the moiré effects range from the subtle to the very obvious, depending upon the collimator being used and the relative orientation of the phantom. Some of the effects may be misleading unless there is a thorough understanding of the conditions under which the images were taken, together with care in their analysis. This must in turn place some limitations upon the use of test objects composed of regular patterns in standard quality assurance programs.

Although the overall effect of moiré interference in these images is disruptive, there are nevertheless some ways in which it may be used in the fields of both quality assurance and performance testing. Three examples are given below.

1. The continuing visibility of moiré fringes and assessment of their sharpness may provide an indirect check on the constancy of the intrinsic spatial resolution of the camera, and would be particularly effective using the 'type 2' fringes arising from a bar phantom aligned parallel to the collimator axis. This is based on the fact that small reductions in gamma camera performance which may not be observable from direct qualitative assessment of the spatial resolution should produce greater changes in the moiré fringe pattern, thus making it a more sensitive indicator.

2. The segment(s) at which moiré effects are first noticeable will provide an approximate measure of the size of the hole-array in what may be a closed collimator system. This could be used to determine the effective resolution limit of the collimator for any imaging application, a figure which may not be obtainable from a single phantom image.

3. Perhaps the most useful aspect of moiré interference effects however would be to provide an initial and continuing check on the physical integrity and quality of collimators. A parallel-line-equal-spacing (PLES) phantom or similar test object would be the method best suited to the qualitative and possibly quantitative analysis of the fringe pattern. It would have a bar size sufficiently small to allow easy visibility of interference fringes. If the phantom is of good quality and the collimator free of defect, the fringe pattern will be even and uniform over the entire field of view. Any damage or defect in the collimator will then produce distortions in the fringe pattern around the area of the defect. A minor example of this can be seen in Fig. 3, where the fringe pattern at the left hand edge of the fifth segment shows slight distortion centrally. This type of application in fact accounts for the major usage of moiré fringes industrially (*8*), and should reveal both superficial and internal defects resulting from manufacture or usage.

In addition, moiré effects have been used in the past (*9*) to provide a bar phantom of continuously variable size, by interfering two parallel line grid sources.

Moiré interference is clearly seen using low-energy collimators of the hole-array type with the present generation of gamma cameras. Any further improvements in their intrinsic spatial resolution would be expected to result in an increase in the visibility of fringe systems, and may also see the beginning of interference effects in cameras with "folded-ribbon" type collimators.

## REFERENCES


1. Bonte FJ, Graham KD, Dowdey JE: Image aberrations produced by multichannel collimators for a scintillation camera. *Radiology* 98:329–334, 1971
2. Bonte FJ, Dowdey JE: Further observations on the septum effect produced by multichannel collimators for a scintillation camera. *Radiology* 102:653–656, 1972
3. Yeh E-L: Distortion of bar phantom images by collimator. *J Nucl Med* 20:260–261, 1979
4. Brown PH, Royal HD: Re: Distortion of bar phantom images by collimator (lett). *J Nucl Med* 20:1100–1101, 1979
5. Johnston RE: Moiré patterns in gamma camera images (lett). *J Nucl Med* 20:1100, 1979
6. Hart GC: The effect of collimator design on moiré patterns in gamma camera bar phantom images. *Phys Med Biol* 29:433–436, 1984
7. Guild J: *The Interference Systems of Crossed Diffraction Gratings*, Oxford University Press, 1956
8. Theocaris PS: Moiré fringes in strain analysis. Pergamon Press, 1969
9. Brunsden BS, et al: A continuously variable line phantom for quality assurance. In *Medical Radionuclide Imaging*, Proceedings of a Symposium, Los Angeles, Oct. 1976, Vol. 1, 1977, p 43